

Alfvén wave support of a dwarf molecular cloud

I. An isothermal model

C.E. Martin¹, J. Heyvaerts², and E.R. Priest¹

¹ School of Mathematical and Computational Sciences, University of St Andrews, North Haugh, St Andrews, Fife KY16 9SS, Scotland

² Observatoire de Strasbourg et Université Louis Pasteur, 11 rue de l'Université, F-6700 Strasbourg, France

Received 14 April 1997 / Accepted 13 May 1997

Abstract. Dwarf (or dark) molecular clouds and molecular clumps have a lifetime which is greater than their dynamical time and must therefore be, in an average sense, in mechanical equilibrium. Equilibrium perpendicular to a global magnetic field is by magnetic forces and it is proposed that along the field the gas is supported by an Alfvén wave pressure force. A self-consistent analytical model, utilising a WKB approximation, is developed for such support. It is found that Alfvén waves are indeed a good candidate for this support, generating model cloud thicknesses consistent with observations. The effect of damping by the linear process of ion-neutral friction is considered. It is found that the damping of the waves is not a necessary condition for the support of the cloud although weak damping is an advantage. The possible sources of these waves are discussed.

Key words: ISM: clouds – ISM: magnetic fields – ISM: structure – MHD – waves

1. Introduction

Molecular clouds are the birth places of stars within our Galaxy. They fall into two categories: giant molecular clouds (GMCs) from which massive stars are formed; and dwarf (or dark) molecular clouds (DMCs) which give low-mass solar-type stars. GMCs are observed to be several tens of parsecs in size with masses $\sim 10^5 - 10^6 M_\odot$ and temperatures $\sim 10\text{K}$. In comparison DMCs have masses $\leq 10^3 M_\odot$ contained within just a few parsecs (radii $\sim 2-5\text{pc}$). See also Shu, Adams & Lizano (1987) and Young & Scoville (1991).

The dynamic giant molecular clouds, probably assembled and dispersed as they cross the spiral arms (Young & Scoville 1991; Scoville 1992), are actually shown by observations of CO emission to be composed of smaller clumps which have physical properties akin to those of dwarf molecular clouds. An example

of such a cloud complex would be the molecular cloud associated with the Orion Nebula (the closest such object to us, at a distance of $\sim 500\text{pc}$) or that associated with the Rosette Nebula (Blitz & Thaddeus 1980). Dwarf molecular clouds themselves are not observed solely within the spiral arms of the Galaxy. They are likely to exist for a period of time greater than that taken to bridge the gap between the arms and thus have lifetimes $\geq 10^8\text{yr}$ (compared to $\sim 10^7\text{yr}$ for GMCs). The most well known of these objects are in Taurus, the closest molecular clouds at a distance of $\sim 140\text{pc}$.

Giant molecular clouds are far from equilibrium. In contrast, dwarf molecular clouds, as well as the clumps in giant cloud complexes, must be near mechanical equilibrium as they have a lifetime which is greater than their dynamical time. They also have a mass greater than their Jeans mass but are not observed to be collapsing.

Consider firstly the time-scales in a self-gravitating molecular cloud. The free-fall collapse (dynamic) time-scale is given by

$$t_{\text{ff}} = \sqrt{3\pi/32G\rho}, \quad (1)$$

where ρ is the mass density and G is the gravitational constant; for a typical number density of $n_{\text{H}_2} \sim 10^9\text{m}^{-3}$ ($\sim 10^3\text{cm}^{-3}$) this yields $t_{\text{ff}} \sim 10^6\text{yr}$, much less than the expected lifetime of a DMC. However, as the cloud is threaded by a magnetic field the ambipolar diffusion time-scale also needs to be considered. This is the time-scale at which the neutral particles diffuse through the magnetic field and charged particles, and is given by

$$t_{\text{AD}} = L^2/\mathcal{D}, \quad (2)$$

where L is the characteristic length-scale of the magnetic field and \mathcal{D} is a diffusion coefficient. The ratio of this diffusion time-scale to the dynamic time-scale may be approximated by the expression

$$t_{\text{AD}}/t_{\text{ff}} \sim \gamma C/2\sqrt{2\pi G} \sim 8, \quad (3)$$

where γ is a drag coefficient and C is a weak function of the gas temperature (see also Sect. 3) (Shu 1983; Shu et al. 1987). Hence

it can be seen that the diffusion time-scale, being in order of magnitude $t_{\text{AD}} \sim 10^7 \text{ yr}$, is slower than that for free-fall collapse but still less than the lifetime of a DMC which is $\sim 10^8 \text{ yr}$ or more.

Secondly, consider the Jeans mass, M_J — the critical mass at which the internal gas pressure is no longer sufficient for hydrostatic support and the cloud will gravitationally collapse — which is given approximately by the expression

$$M_J \sim (k_B T / \bar{m} G)^{\frac{3}{2}} \rho^{-\frac{1}{2}}, \quad (4)$$

where k_B is the Boltzmann constant, T is the temperature, \bar{m} is the mean molecular weight, G is the gravitational constant and ρ is the mass density. For a typical temperature and number density of 10K and $\sim 10^9 \text{ m}^{-3}$ ($\sim 10^3 \text{ cm}^{-3}$), respectively, this gives $M_J \sim 3M_\odot$, clearly implying that in typical dwarf molecular clouds $M_J \ll M_{\text{cloud}}$ and the cloud should, in the absence of other influences such as turbulence or magnetic fields, be undergoing free-fall collapse. However, if all of the dark clouds within the Galaxy were undergoing free-fall collapse then the predicted star formation rate (SFR) would be larger than the actual rate, of $\sim 3 - 5M_\odot \text{ yr}^{-1}$, by a factor of $\sim 10 - 100$ depending on the amount of mass assumed to be contained within these clouds (see also Zuckerman & Palmer 1974; Field 1978; Shu et al. 1987).

Having shown explicitly that dwarf molecular clouds have both a lifetime greater than their dynamical time and a mass which is greater than their Jeans mass, attention needs to be given to the mechanism by which these clouds are supported against their own gravity.

If the mechanical equilibrium of a self-gravitating cloud is determined solely by the internal gas pressure (P) and gravity (\mathbf{g}) then the equilibrium equation would be $\nabla P = \rho \mathbf{g}$, where ρ is the mass density. For an isothermal layer with $P(z) = \rho(z)c^2$, where c is the sound speed, such an equilibrium would give the density profile

$$\rho/\rho_0 = \text{sech}^2(z/H) \quad (5)$$

(see also Spitzer 1968), where $H = c^2/(\pi G \mathcal{M})$ is a scale-height and \mathcal{M} is the column density. For a typical dwarf molecular cloud with mass $100M_\odot$ and radius 1pc the column density is $\mathcal{M} \approx 10^{-1} \text{ kg m}^{-2}$, which together with a temperature $T = 10\text{K}$ gives $H \approx 0.1\text{pc}$. This scale-height suggests that the isothermal layer would be akin to a “flattened pancake”¹, which is inconsistent with observations of dwarf molecular clouds (e.g. see Shu et al. 1987).

In conclusion, all of the evidence presented here clearly indicates the need for some additional support against the self-gravity of the dwarf molecular cloud (or clump within a giant cloud complex). This support would act to hinder gravitational collapse and hence a flattened pancake morphology.

¹ It is important to note that this description of DMCs would also apply to more realistic geometries since the magnetic field threading the cloud would provide support perpendicular to its direction via the Lorentz force.

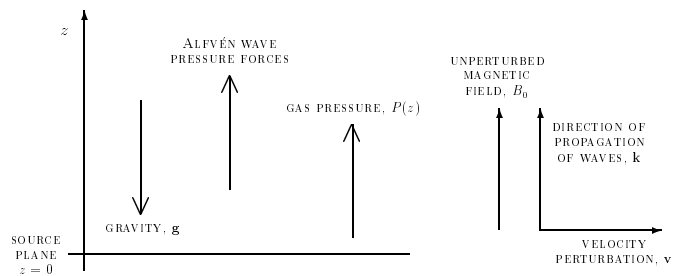


Fig. 1. A representation of the model showing the Alfvén wave pressure force and the gas pressure counteracting the gravity

There have been many candidates for this support discussed by various authors over the years. These include rotation (Field 1978), internal cloud hydrodynamic turbulence (Bonazzola et al. 1987, 1992), turbulence via stellar outflows (Norman & Silk 1980; McKee 1989), and magnetic fields and the waves which they support (Arons & Max 1975; Shu et al. 1987; Fatuzzo & Adams 1993; McKee & Zweibel 1995; Gammie & Ostriker 1996). Of these, magnetic fields offer a great deal of promise. They have been observed to be ordered on the scale of molecular clouds (Moneti et al. 1984; Goodman & Heiles 1994) with field strengths, measured by the Zeeman effect in OH (e.g. Crutcher & Kazès 1983) and HI (e.g. Goodman & Heiles 1994), to be in the region of $\sim 1 - 10 \text{ nT}$ ($\sim 10 - 100 \mu\text{G}$). For typical densities of $\sim 10^9 \text{ m}^{-3}$ ($\sim 10^3 \text{ cm}^{-3}$) and a field strength of $\sim 10 \text{ nT}$ the Alfvén speed is calculated to be $v_A \sim 4.5 \text{ km s}^{-1}$, which compares to a sound speed, with a temperature 10K, of $c \sim 0.25 \text{ km s}^{-1}$ and fluid motions, measured from CO linewidths (Shu et al. 1987), of $\sim 1 \text{ km s}^{-1}$. Such values show that a dwarf molecular cloud is a low- β environment with fluid velocities that are supersonic but subalfvénic.

It is difficult for supersonic turbulence to explain these linewidths or indeed to provide support for the cloud in the form of a turbulent pressure as it is highly dissipative (e.g. see Field 1978; Shu et al. 1987). In contrast, magnetic fields and the hydromagnetic waves they support are not easily dissipated. They imply a linewidth-size relation which is in agreement with observations (Arons & Max 1975; Mouschovias & Psaltis 1995) and so again look favourable for cloud support. Now, any disturbance within the cloud would generate magnetohydrodynamic (MHD) waves, the longest-lived being the Alfvén wave (Zweibel & Josafatsson 1983), which would act on the background gas like an anisotropic pressure force (Dewar 1970). Hence, within this work it is proposed that a dwarf (or dark) molecular cloud is supported perpendicular to the ordered magnetic field by the Lorentz force and parallel to the field by Alfvén wave pressure.

The extent of the support perpendicular to the field can be described in terms of a critical mass, M_{crit} , above which the magnetic support would fail and the cloud would undergo gravitational collapse. This mass,

$$M_{\text{crit}} = 5 \times 10^5 M_\odot \left(\frac{B}{3 \mu\text{G}} \right)^3 \left(\frac{n_p}{1 \text{ cm}^{-3}} \right)^{-2}, \quad (6)$$

where B is the magnetic field and n_p is the number density of protons, is determined from calculations of the equilibria of isothermal, self-gravitating clouds with a frozen-in magnetic flux (Mouschovias & Spitzer 1976; Mouschovias 1995).

The structure of this paper is as follows: the equations of the model will be developed in Sect. 2, while Sect. 3 will discuss Alfvén waves in such interstellar media. The results will be presented and discussed in Sect. 4 and then concluded in Sect. 5.

2. The model

Within this study a dwarf molecular cloud is modelled as a one-dimensional slab where the gravity, which acts to collapse the cloud, is opposed by the internal gas pressure and the Alfvén wave pressure force (see Fig. 1). In this first approach it is assumed that the Alfvén waves are emitted from the innermost part of the cloud, the wave sources being located in the central plane. The model is currently being improved to allow for a more realistic source distribution.

All of the gradients are in the z -direction, the central source plane being at $z = 0$, such that the mass density $\rho = \rho(z)$; the gravitational acceleration $\mathbf{g} = -g(z)\hat{\mathbf{z}}$; the plasma velocity $\mathbf{v} = v(z, t)\hat{\mathbf{x}}$; the magnetic field

$$\mathbf{B} = B_0\hat{\mathbf{z}} + b(z, t)\hat{\mathbf{x}}; \quad (7)$$

and the gas pressure $P(z) = \rho(z)c^2$, where the gas is assumed to be isothermal with a sound speed c . The velocity perturbation $v(z, t)$ is taken to be Alfvénic in nature and is therefore perpendicular to the direction of the applied uniform magnetic field B_0 . The associated magnetic perturbation is $b(z, t)$. Such wave motions do not induce any compression in the gas, which is treated as one-fluid (the neutrals and ions being taken together).

2.1. Equations of the model

In a magnetohydrodynamic model (e.g. Priest 1982) the equation of motion including gravity is

$$\rho \frac{\partial \mathbf{v}}{\partial t} + \rho (\mathbf{v} \cdot \nabla) \mathbf{v} = -\nabla P + (\mathbf{B} \cdot \nabla) \frac{\mathbf{B}}{\mu} - \nabla \left(\frac{B^2}{2\mu} \right) + \rho \mathbf{g}, \quad (8)$$

where ρ is the mass density, \mathbf{v} is the velocity, P is the pressure, \mathbf{g} is the gravity, \mathbf{B} is the magnetic field and μ is the magnetic permeability of free space.

For wave periods shorter than the characteristic free-fall time, which is normally longer than the fundamental Alfvén wave period in a low- β plasma, this equation can be averaged over time. The result is an equilibrium equation (or force-balance equation) between the gravity, the gas pressure and the pressure exerted by the Alfvén waves,

$$0 = -\nabla P - \nabla \left\langle \frac{b^2(z, t)}{2\mu} \right\rangle + \rho \mathbf{g}, \quad (9)$$

where $b(z, t)$ is the magnetic field perturbation. Since all of the components of this equation are functions of z only, the equilibrium equation can be written

$$\frac{dP}{dz} + \frac{d}{dz} \left\langle \frac{b^2}{2\mu} \right\rangle = -\rho g. \quad (10)$$

The motion of the MHD wave is described by the equation of motion

$$\rho \frac{\partial v}{\partial t} - \frac{B_0}{\mu} \frac{\partial b}{\partial z} = 0. \quad (11)$$

Note that there is no explicit linearisation involved in determining Eqs. (10) and (11); the form of the velocity (v) and the associated magnetic field perturbation (b) leave the Alfvén wave pressure as the single non-linear term. The wave acts directly on the ions and electrons in the cloud with the neutrals (n) supported, in turn, by the friction force that they exert on the ions (i),

$$\mathbf{f}_{n \rightarrow i} = -\rho_i \rho_n \gamma (\mathbf{v}_i - \mathbf{v}_n) \quad (12)$$

(Shu et al. 1987). Thus a term appears in the equation of motion which represents the friction between the neutrals and ions, giving

$$\rho \frac{\partial v}{\partial t} = \frac{B_0}{\mu} \frac{\partial b}{\partial z} - \Gamma \rho v, \quad (13)$$

where Γ is the damping rate (see also Sect. 3).

In the perfectly conducting limit the induction equation becomes

$$\frac{\partial \mathbf{B}}{\partial t} = \nabla \times (\mathbf{v} \times \mathbf{B}), \quad (14)$$

which, when taken with Eq. (7) and $\mathbf{v} = v(z, t)\hat{\mathbf{x}}$, reduces to

$$\frac{\partial b}{\partial t} = B_0 \frac{\partial v}{\partial z}. \quad (15)$$

The magnetic perturbation ($b(z, t)$) can be eliminated from Eq. (13) by differentiating it with respect to time (t) and using Eq. (15) to give the wave propagation equation

$$\frac{\partial^2 v}{\partial t^2} = v_A^2 \frac{\partial^2 v}{\partial z^2} - \Gamma \frac{\partial v}{\partial t}, \quad (16)$$

where $v_A = B_0/\sqrt{\mu\rho}$ is the Alfvén speed.

Assuming harmonic wave motion allows both the velocity and magnetic perturbations to be written as

$$v(z, t) = \Re(\tilde{v}(z) e^{-i\omega t}), \quad b(z, t) = \Re(\tilde{b}(z) e^{-i\omega t}),$$

where ω is the frequency and \tilde{v}, \tilde{b} are the complex wave amplitudes

$$\tilde{v}(z) = v_1(z) + iv_2(z), \quad \tilde{b}(z) = b_1(z) + ib_2(z).$$

Thus, upon substitution, Eq. (16) becomes

$$v_A^2 \frac{d^2 \tilde{v}}{dz^2} + \omega^2 \tilde{v} + i\Gamma\omega\tilde{v} = 0, \quad (17)$$

and similarly Eq. (15) is now

$$-i\omega\tilde{b} = B_0 \frac{d\tilde{v}}{dz}. \quad (18)$$

The corresponding time-averaged wave pressure is

$$\langle b^2(z, t) \rangle = (b_1^2 + b_2^2)/2, \quad (19)$$

thus allowing the equilibrium equation to be written as

$$\frac{d}{dz} \left(\rho c^2 + \frac{b_1^2 + b_2^2}{4\mu} \right) = -\rho g, \quad (20)$$

where the gas pressure $P = \rho c^2$. The model is described by this equation together with the wave propagation equations (Eqs. 17 and 18) and the self-gravitation equation

$$\frac{dg}{dz} = 4\pi G\rho. \quad (21)$$

2.2. WKB waves

The WKB approximation is a method for solving wave equations in a non-uniform medium which is varying over a scale much larger than the wavelength of the waves. In the case where the wavelengths of the Alfvén waves are short compared with the size of the cloud, this approximation can be applied to the wave equations calculated above.

Consider Eqs. (17) and (18) and let the wave amplitude \tilde{v} be written as $\tilde{v}(z) = \mathcal{V}(z) e^{i\phi(z)}$, where $\phi(z)$ is varying at a faster rate than $\mathcal{V}(z)$, such that

$$v_A^2 (-\mathcal{V}'\phi'^2 + i\mathcal{V}'\phi'' + 2i\mathcal{V}'\phi') + \omega^2 \mathcal{V} + i\Gamma\omega\mathcal{V} = 0, \quad (22)$$

(where $'$ indicates a derivative with respect to z) which on equating the real and imaginary terms gives

$$\phi' = \omega/v_A, \quad (23)$$

and

$$\frac{d}{dz} \left[\ln(\phi' \mathcal{V}^2) \right] = -\frac{\Gamma}{v_A}. \quad (24)$$

Now let $\tilde{b}(z) = \mathcal{B}(z) e^{i\phi(z)}$ to give

$$\mathcal{B} = -(B_0 \mathcal{V}' \phi') / \omega. \quad (25)$$

But,

$$\frac{d}{dz} \left[\ln(\mathcal{V}^2) \right] = \frac{d}{dz} \left[\ln \left(\frac{\mathcal{B}^2}{\phi'^2} \right) \right] \quad (26)$$

as ω and B_0 are constants. Substituting this into Eq. (24) and using $\phi' = \omega/v_A$ (Eq. 23), reduces the wave propagation equations to just one, namely

$$\frac{d}{dz} \left[\ln \left(\frac{\mathcal{B}^2}{\sqrt{\rho}} \right) \right] = -\frac{\Gamma}{v_A}. \quad (27)$$

In the particular case of WKB waves the wave pressure term becomes

$$\langle b^2(z) \rangle = \mathcal{B}^2/2, \quad (28)$$

and thus the equilibrium equation (Eq. 10) is

$$\frac{d}{dz} \left(\rho c^2 + \frac{\mathcal{B}^2}{4\mu} \right) = -\rho g. \quad (29)$$

2.2.1. The wave energy density

Within a WKB approximation and a steady state the wave energy density obeys an equation of radiative transfer which, in regions where no waves are emitted, can be simply written in the form

$$\nabla \cdot (\epsilon \mathbf{v}_g) = -\kappa_v \epsilon, \quad (30)$$

where ϵ is the energy density, κ_v is the volume absorption coefficient and \mathbf{v}_g is the group velocity. In comparison, letting $U = \mathcal{B}^2/4\mu$ simply reduces Eq. (27) to the Alfvén wave energy transport equation (Eq. 30). This shows that U is the wave energy density, noting that in an Alfvén wave energy is transmitted partly as magnetic energy ($B^2/2\mu$) and partly as kinetic energy ($\rho v^2/2$), the electrical energy being insignificant.

Thus the equations describing the model have been reduced to just three within this WKB approximation: the wave equation

$$\frac{d}{dz} \left(\frac{U}{\sqrt{\rho/\rho_0}} \right) = -\frac{\Gamma}{v_{A0}} U; \quad (31)$$

the equilibrium equation

$$\frac{d}{dz} (\rho c^2 + U) = -\rho g; \quad (32)$$

and the self-gravitation equation (Eq. 21)

$$\frac{dg}{dz} = 4\pi G\rho.$$

These are the equations which will be solved in Sect. 4, together with the boundary conditions $U = U_0$, $\rho = \rho_0$, $g = 0$ at $z = 0$. The first of these conditions reflects the assumption that the Alfvén waves are emitted from the central plane. The value of the central mass density together with that for the central wave energy density are determined from the column density of the gas layer. The relation between these parameters will be calculated a posteriori.

3. Alfvén waves in a weakly ionized cloud

A dwarf (or dark) molecular cloud is a weakly ionized environment, the mass of the ionized part being $\sim 10^{-6}$ that of the neutral mass. However, the Alfvén waves acting to support the cloud will only act directly on the electric component. Thus in order for the cloud to be supported as a whole there needs to be very good coupling between the ions and neutrals within the cloud. If this were not the case the electric component of the cloud would still be supported but the neutral mass (by far the greater part of the cloud) would not, hence giving the cloud a flattened pancake morphology (as in Sect. 1). This coupling is provided by the friction exerted on the ions by the neutrals, which is given by the expression (Eq. 12)

$$\mathbf{f}_{n \rightarrow i} = -\rho_i \rho_n \gamma (\mathbf{v}_i - \mathbf{v}_n),$$

where ρ_i , ρ_n and \mathbf{v}_i , \mathbf{v}_n are the mass densities and velocities of the ions and neutrals, respectively, and $\gamma = 3.5 \times 10^{13} \text{cm}^3 \text{g}^{-1} \text{s}^{-1}$ is a drag coefficient (Draine et al. 1983; Shu et al. 1987).

Consider the equation of motion for the waves (Eq. 13) within a two-fluid (ions and neutrals) analysis including the ion-neutral friction explicitly,

$$\rho_i \frac{\partial v_i}{\partial t} = \frac{B_0}{\mu} \frac{\partial b}{\partial z} - \rho_i \rho_n \gamma (v_i - v_n), \quad (33)$$

$$\rho_n \frac{\partial v_n}{\partial t} = \rho_i \rho_n \gamma (v_i - v_n), \quad (34)$$

where subscript n corresponds to the neutral quantities and i the ionic quantities. Within this regime the induction equation becomes

$$\frac{\partial b}{\partial t} = B_0 \frac{\partial v_i}{\partial t}. \quad (35)$$

If the wave motions are assumed to be of the form $\exp(i(kz - \omega t))$ where k is the wavenumber and ω the angular frequency, then Eqs. (33), (34) and (35), become

$$-i\omega \rho_i v_i = (B_0/\mu) ikb - \rho_i \rho_n \gamma (v_i - v_n) \quad (36)$$

$$-i\omega \rho_n v_n = \rho_i \rho_n \gamma (v_i - v_n) \quad (37)$$

$$-i\omega b = B_0 ikv_i \quad (38)$$

and can be used to determine the dispersion relation, viz:

$$k^2 v_{Ai}^2 = \omega^2 \left(1 + \frac{\rho_n \gamma}{\rho_i \gamma - i\omega} \right), \quad (39)$$

where $v_{Ai} = B_0/\sqrt{\mu \rho_i}$ is the ion Alfvén speed.

The extent of the coupling between the ions and neutrals within the cloud is dependent upon the wave frequency ω , for which there are two limiting cases:

$$(a) \omega \gg \rho_i \gamma; \omega \gg \rho_n \gamma$$

From Eq. (37) it can be seen that

$$v_n = v_i \left(\frac{\rho_i \gamma}{\rho_i \gamma - i\omega} \right), \quad (40)$$

which in this limiting case shows that $v_n \ll v_i$ and hence the neutrals are not well coupled to the ions.

$$(b) \omega \ll \rho_i \gamma$$

In contrast this limit implies, by Eq. (40), that $v_n \simeq v_i$ and hence the coupling between the neutrals and ions is very good, allowing the MHD waves to support the cloud as a whole. In this limit, where there is no difference between the mean velocity of the ions and that of the neutrals, the induction equation (Eq. 35) reduces to Eq. (15) thus justifying this equation within the single fluid approximation.

Comparing these two limits the maximum value the wave frequency can take, while still allowing some coupling between the electric and neutral components of the molecular cloud, is

$$\omega_{\max} = \rho_i \gamma = \rho_n \xi \gamma, \quad (41)$$

where ξ is the ionized mass fraction. For a cosmic-ray ionization rate of $\zeta = 10^{-17} \text{s}^{-1}$ this takes a value of

$$\xi = \frac{\rho_i}{\rho_n} = 4.84 \times 10^{-6} \left(\frac{n_{\text{H}_2}}{10^9 \text{m}^{-3}} \right)^{-\frac{1}{2}} \quad (42)$$

using $\rho_n = 2.3 m_{\text{H}} n_{\text{H}_2}$ (Shu et al. 1987; Mouschovias 1995) and $\rho_i = C \sqrt{\rho_n}$, where for average metal depletions and low temperatures $C = 3 \times 10^{-16} \text{cm}^{-3} \text{g}^{\frac{1}{2}}$ (Elmegreen 1979; Shu et al. 1987). The maximum wave frequency gives a minimum wave period of

$$\tau_{\min} = \frac{2\pi}{\omega_{\max}} = 3.06 \times 10^5 \text{yr} \left(\frac{n_{\text{H}_2}}{10^9 \text{m}^{-3}} \right)^{-\frac{1}{2}} \quad (43)$$

and so waves which have a period much less than 10^5yr do not contribute to the MHD wave support of the whole cloud, regardless of the degree to which they are damped.

It is important to note explicitly the dependence of this wave period on the ionization fraction of the cloud: $\tau_{\min} \propto \xi^{-1} \propto \zeta^{-1/2}$ (Elmegreen 1979). The value adopted for the ionization rate in Eq. (42) gives a very low ionized mass fraction which is thought to be typical in these clouds (Shu et al. 1987; Hartquist & Williams 1995). However the value of τ_{\min} can be affected by a variation in the cosmic-ray ionization rate (Farquhar et al. 1994) as well as embedded or external sources of ultraviolet or x-ray radiation (Gredel et al. 1989; Le Bourlot et al. 1993; Tiné et al. 1997; Yan & Dalgarno 1997) depending upon the location and point of evolution of the cloud (Hartquist et al. 1993). Such sources yield x-ray dominated regions (XDRs) (e.g. Tiné et al. 1997) and photodissociation regions, or photon dominated regions (PDRs), (e.g. Le Bourlot et al. 1993) in which the ionization rate may be substantially increased. For example, an ionization rate of $\zeta = 10^{-12} \text{s}^{-1}$, for typical number densities of $\sim 10^9 \text{m}^{-3}$, (Tiné et al. 1997) reduces the minimum wave period (τ_{\min}) to $\sim 10^3 \text{yr}$.

Considering these waves still further leads to the introduction of a maximum wave period, τ_{\max} ; the wavelength of the MHD wave must be less than the size of the cloud given that the fundamental mode must have a wavelength of that order,

and also because such a long wavelength would offer only very little support to the gas. Thus, $\tau_{\max} = R_c/v_A$ is given by

$$\tau_{\max} = 1.07 \times 10^6 \text{yr} \left(\frac{R_c}{5\text{pc}} \right) \left(\frac{10\text{nT}}{B} \right) \left(\frac{n_{\text{H}_2}}{10^9 \text{m}^{-3}} \right)^{\frac{1}{2}}, \quad (44)$$

where R_c is the radius (or thickness in this model) of the cloud and v_A is the Alfvén speed of the neutrals and ions together which is given by

$$v_A = 4.55 \text{km s}^{-1} \left(\frac{B}{10\text{nT}} \right) \left(\frac{n_{\text{H}_2}}{10^9 \text{m}^{-3}} \right)^{-\frac{1}{2}}. \quad (45)$$

In the limit where there is good coupling between the ions and neutrals (case (b)) the dispersion relation (Eq. 39), using a Taylor series expansion, becomes

$$k v_A \simeq \pm \omega \left(1 + \frac{i}{2} \frac{\omega \rho_n}{(\rho_i + \rho_n) \rho_i \gamma} \right), \quad (46)$$

where $v_A = B_0/\sqrt{\mu(\rho_i + \rho_n)}$. Thus it is possible to define a damping rate, for a wave to damp by a factor e , as

$$\Gamma = k_i v_A = \frac{1}{2} \frac{\omega^2 \rho_n}{(\rho_i + \rho_n) \rho_i \gamma}, \quad (47)$$

where k_i is the imaginary term in the dispersion relation. Given that the ionized mass fraction is so small (Eq. 42) the damping rate can be written as

$$\Gamma = \frac{1}{2} \frac{\omega^2}{\xi \rho_n \gamma} \quad (48)$$

to a very good approximation. In terms of the wave period (τ) and the molecular hydrogen number density (n_{H_2}) this parameter has a value of

$$\Gamma = 9.61 \times 10^{-5} \text{yr}^{-1} \left(\frac{n_{\text{H}_2}}{10^9 \text{m}^{-3}} \right)^{-\frac{1}{2}} \left(\frac{\tau}{10^5 \text{yr}} \right)^{-2}, \quad (49)$$

corresponding to a damping time of

$$t_d = \frac{1}{\Gamma} = 1.04 \times 10^4 \text{yr} \left(\frac{n_{\text{H}_2}}{10^9 \text{m}^{-3}} \right)^{\frac{1}{2}} \left(\frac{\tau}{10^5 \text{yr}} \right)^2 \quad (50)$$

and a damping length of

$$l = v_A t_d = 4.84 \times 10^{-2} \text{pc} \left(\frac{B}{10\text{nT}} \right) \left(\frac{\tau}{10^5 \text{yr}} \right)^2. \quad (51)$$

The ion-neutral friction relied upon to couple the two components of the cloud is also a linear process acting to dampen the MHD waves propagating through the cloud. Zweibel & Josafatsson (1983) suggest that the most effective damping mechanism is non-linear steepening of the waves into shocks, caused by the wave magnetic pressure gradient, followed by linear ion-neutral friction. For waves which propagate parallel to the unperturbed magnetic field the damping rate for this non-linear effect is found to be

$$\Gamma_{\text{NL}} = \frac{\omega \delta v^2}{v_A^2} \quad (52)$$

(Zweibel & Josafatsson 1983), where δv is the turbulent fluid velocity. This corresponds to a damping length of

$$l_{\text{NL}} = 1.53 \text{pc} \left(\frac{n_{\text{H}_2}}{10^9 \text{m}^{-3}} \right)^{-\frac{3}{2}} \left(\frac{B}{10\text{nT}} \right)^3 \times \left(\frac{\tau}{10^5 \text{yr}} \right) \left(\frac{\delta v}{1 \text{km s}^{-1}} \right)^{-2} \quad (53)$$

for typical parameters within this study. Now the non-linear damping process will completely dominate the linear process if $l_{\text{NL}} \ll l$. This is generally not the case for realistic fluid velocities (e.g. see Myers & Goodman 1988 and references therein) and so the damping within this model is taken to be solely by the linear process of ion-neutral friction.

3.1. The source of the waves

The required efficiency of the ion-neutral coupling results in a minimum period for waves supporting the cloud of $\sim 10^5 \text{yr}$ for a typical ionization fraction. Which source within a dwarf molecular cloud could generate waves of this period? Of course, any motion not parallel to the direction of the unperturbed magnetic field will generate waves, but consider in turn: an expanding HII region (Arons & Max 1975); and the orbital motions within the gas as a whole, namely, large-scale (Falgarone & Puget 1986) or protostellar condensations (Arons & Max 1975).

The first of these possible sources, the Strömgren sphere, is unlikely to prove viable within the environment of a DMC as these clouds produce low-mass stars which are not strongly ionizing. In addition, this source would only be available in clouds with embedded stars and thus could not provide support for a quiescent dwarf cloud which had not yet formed any stars.

Secondly, consider the orbital motions of the clumps and cores (Hartquist et al. 1993) within the cloud. Kepler's third law states that

$$\tau_K^2 = \frac{4\pi^2}{GM} R^3, \quad (54)$$

where τ_K is the period, G is the gravitational constant, M is the mass and R is the orbital radius. Larson (1981) first showed there to be a correlation between the observed mass densities and sizes of molecular clumps, which states approximately that

$$\frac{M_{\text{clump}}}{100 M_{\odot}} = \frac{R_{\text{clump}}^2}{1 \text{pc}} \quad (55)$$

(e.g. see Falgarone & Puget 1986) and allows Eq. (54) to be written

$$\tau_K = 9.37 \times 10^6 \text{yr} \left(\frac{R_{\text{clump}}}{1 \text{pc}} \right)^{\frac{1}{2}}. \quad (56)$$

Hence for large-scale condensations within a molecular cloud $R_{\text{clump}} \sim 0.1 \text{pc}$, say, the period is $\tau_K \sim 3 \times 10^6 \text{yr}$, which is greater than the calculated minimum period of $\sim 10^5 \text{yr}$ and thus represents a viable source for the waves providing the support.

Decreasing the size of the clump down to the typical size of a protostellar core, $1M_{\odot}$ in 100AU say, reduces the period to just $\sim 10^3$ yr. This would appear to suggest that the orbital motions of cores do not represent a useful source if the ionization fraction is given by Eq. (42). However if the ionization rate is increased, say by an embedded star within the core (as discussed above), then these cores could act as an additional source for the Alfvén waves.

This section has discussed the wave sources available in a DMC and shown them to be the motions of condensations in the cloud. Within the slab geometry utilised in this paper it has been assumed that these denser regions of gas lie along the central plane of the layer ($z = 0$), thus simplifying the probable distribution of clumps and cores within a DMC.

4. Alfvén wave support

The set of equations fully describing the model (Eqs. 31, 32 and 21) will now be solved to give the density profile and hence the “thickness” of the layer, in two cases: without any wave damping; and including wave damping in accordance with ion-neutral friction.

4.1. Without damping

In the absence of damping, i.e. when $\Gamma = 0$, the WKB wave equation (Eq. 31) implies that

$$U = U_0 \sqrt{\rho/\rho_0}, \quad (57)$$

where ρ_0 and U_0 are the mass and energy densities at the central plane, respectively. Substituting this expression for the wave energy density into the equilibrium equation (Eq. 32) leaves

$$c^2 \frac{d\rho}{dz} + U_0 \frac{d}{dz} \left(\sqrt{\frac{\rho}{\rho_0}} \right) = -\rho g, \quad (58)$$

which together with the self-gravitation equation (Eq. 21) can be used to find the relationship between the gravity (g) and the mass density (ρ). Now Eq. (21) gives an expression for dz which on substituting into Eq. (58) and integrating gives

$$(1 - \sqrt{\tilde{\rho}})(1 + \lambda + \sqrt{\tilde{\rho}}) = g^2/8\pi G\rho_0 c^2, \quad (59)$$

where $\tilde{\rho} = \rho/\rho_0$ and

$$\lambda = U_0/\rho_0 c^2 \quad (60)$$

(see Sect. 4.3 for a discussion of the values of this parameter). This can then be inserted back into Eq. (21) to give the density stratification, which, upon letting $u = \sqrt{(1 - \sqrt{\tilde{\rho}})(1 + \lambda + \sqrt{\tilde{\rho}})}$, becomes

$$z = \frac{2c}{\sqrt{8\pi G\rho_0}} \int_0^s \frac{du}{\left[\sqrt{(1 + \frac{\lambda}{2})^2 - u^2 - \frac{\lambda}{2}} \right]^2}. \quad (61)$$

Applying the substitution $u = (1 + \lambda/2)(2t/1 + t^2)$ gives finally

Table 1. The central mass density (ρ_0), central energy density (U_0) and thickness of an isothermal gas slab supported by waves without damping, with column density $\mathcal{M} = 10^{-1} \text{kg m}^{-2}$ and temperature $T = 10\text{K}$, for increasing values of the parameter λ ; where $\lambda = U_0/\rho_0 c^2$ is the ratio between the wave pressure and the isothermal gas pressure at the central plane ($z = 0$)

| λ | ρ_0 (kg m^{-3}) | U_0 (J m^{-3}) | Thickness (pc) |
|-----------|---------------------------------|-----------------------------|----------------|
| 0 | 1.75×10^{-17} | 0 | 0.20 |
| 10 | 1.59×10^{-18} | 9.52×10^{-13} | 1.84 |
| 20 | 8.33×10^{-19} | 9.98×10^{-13} | 3.49 |
| 30 | 5.64×10^{-19} | 1.01×10^{-12} | 5.13 |
| 40 | 4.27×10^{-19} | 1.02×10^{-12} | 6.77 |

$$z = \frac{2c(1 + \frac{\lambda}{2})}{\sqrt{8\pi G\rho_0}} \left[\frac{\frac{\lambda}{2}}{1 + \lambda} \frac{\sqrt{(1 - \sqrt{\tilde{\rho}})(1 + \lambda + \sqrt{\tilde{\rho}})}}{(1 + \frac{\lambda}{2})\sqrt{\tilde{\rho}}} + \frac{1 + \frac{\lambda}{2}}{(1 + \lambda)^{\frac{3}{2}}} \ln \left\{ \frac{\sqrt{1 + \lambda + \sqrt{\tilde{\rho}}} + \sqrt{(1 + \lambda)(1 - \sqrt{\tilde{\rho}})}}{\sqrt{1 + \lambda + \sqrt{\tilde{\rho}}} - \sqrt{(1 + \lambda)(1 - \sqrt{\tilde{\rho}})}} \right\} \right]. \quad (62)$$

This expression fully describes the relationship between the mass density ratio ($\tilde{\rho}$) and the height above the central plane (z) where $\tilde{\rho} = 1$ at $z = 0$ and $\tilde{\rho} \rightarrow 0$ as $z \rightarrow \infty$. Note that the magnetisation parameter λ is inversely proportional to the plasma beta (β) and therefore larger values of λ correspond to the magnetic field becoming increasingly dominant within the cloud dynamics.

Shown in Table 1 is the thickness of an isothermal gas slab with column density $\mathcal{M} = 10^{-1} \text{kg m}^{-2}$ and temperature $T = 10\text{K}$, for increasing values of λ . The case $\lambda = 0$ represents a cloud in which there is no wave support and hence the gravity is balanced by the internal gas pressure alone (see also Sect. 1). The column density \mathcal{M} is given by the expression

$$\mathcal{M} = \frac{2}{\sqrt{2\pi G}} \sqrt{\rho_0 c^2 (1 + \lambda)} \quad (63)$$

and the thickness of the slab is defined as twice the height above the central plane at which the central mass density has decreased by a factor of e , i.e. $2 \times z(\tilde{\rho} = 1/e)$.

Figure 2 shows simply that increasing the value of the parameter λ , i.e. increasing the wave support, increases the thickness of the isothermal gas slab. Maintaining the same column density requires the mass density at the central plane to decrease as wave support increases (see Fig. 3) so that the material in the layer becomes more evenly distributed. Altering the column density and temperature naturally brings about a change in the thickness of the slab. For example, increasing the column density will favour gravity and hence reduce the size of the slab, whereas increasing the temperature will favour the gas pressure and so increase the thickness. As can be seen from Eq. (62) and Fig. 4, there is a linear relationship between the height (z) above the central plane and the parameter λ , showing that a higher temperature together with a lower column density would increase the thickness of the layer more markedly as the value of λ is increased.

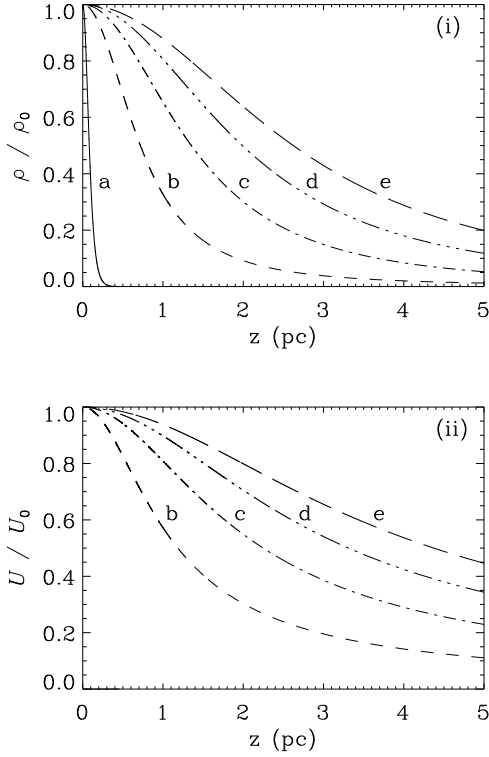


Fig. 2. The (i) mass density ratio and (ii) energy density ratio profiles in an isothermal gas slab supported by waves without damping, with column density $\mathcal{M} = 10^{-1} \text{ kg m}^{-2}$ and temperature $T = 10\text{K}$, for (a) $\lambda = 0$, (b) $\lambda = 10$, (c) $\lambda = 20$, (d) $\lambda = 30$ and (e) $\lambda = 40$; where $\lambda = U_0 / \rho_0 c^2$ is the ratio between the wave pressure and the isothermal gas pressure at the central plane ($z = 0$)

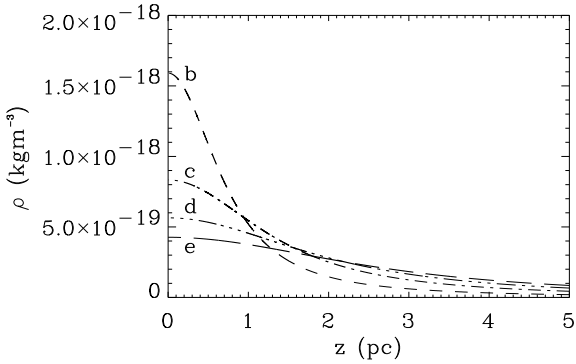


Fig. 3. The mass density profiles as for Fig. 2

Hence, it can be seen from these results that damping is not a prerequisite for the Alfvén waves to support a molecular cloud out to typical observed radii, providing the value of λ and hence the magnitude of the magnetic field perturbation is large enough. The wave flux ($\sim U v_A$) is conserved along the direction of propagation but the Alfvén speed (v_A) is not and so it is the resulting gradient in the wave energy density (U) (see Fig. 2) that provides the support.

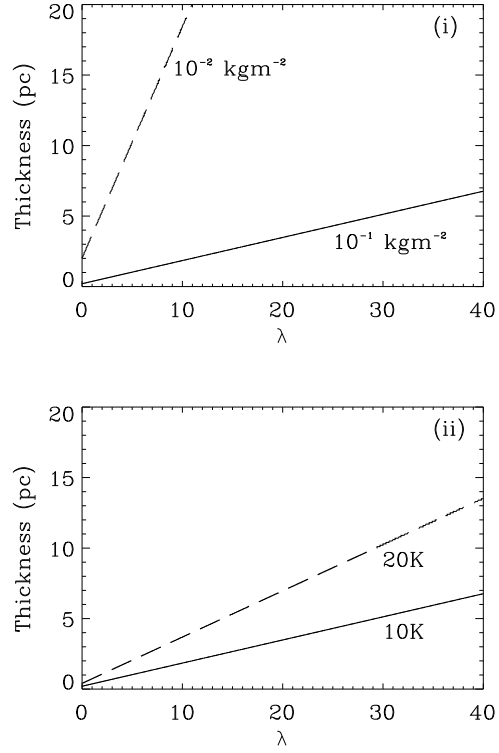


Fig. 4. The thickness of an isothermal gas slab supported by waves without damping plotted against the parameter λ for (i) different values of the column density (\mathcal{M}) with temperature $T = 10\text{K}$ and (ii) different values of the temperature (T) with column density $\mathcal{M} = 10^{-1} \text{ kg m}^{-2}$

4.2. With damping

Friction between the ions and neutrals is the mechanism by which the dwarf molecular cloud is supported as a whole (given that the magnetic field will act directly on the electric component of the cloud and not the neutrals). This ion-neutral friction is a linear process which will act to damp the Alfvén waves propagating through the layer (see also Sect. 3 and Zweibel & Josafatsson 1983).

In the limit when there is good coupling between the ions and the neutrals ($\omega \ll \rho_i \gamma$) the damping rate is given by Eq. (48), where the total mass density $\rho \simeq \rho_n$, which can be written as

$$\Gamma = \kappa / \sqrt{\rho / \rho_0}, \quad (64)$$

where $\kappa = \omega^2 / 2C\gamma\sqrt{\rho_0}$. Using this expression for the damping rate, the WKB wave equation (Eq. 31) integrates to

$$U = U_0 \sqrt{\bar{\rho}} e^{-kz}, \quad (65)$$

where $k = \kappa \sqrt{\mu \rho_0} / B_0$.

As in the previous section, using the self-gravitation equation (Eq. 21) to eliminate the gravity (g) from the equilibrium equation (Eq. 32) gives an expression describing the density stratification

Table 2. The thickness of an isothermal gas slab with column density $\mathcal{M} = 10^{-1} \text{kg m}^{-2}$ and temperature $T = 10\text{K}$ for increasing values of the parameters λ and k ; where $\lambda = U_0/\rho_0 c^2$ is the ratio between the wave pressure and the isothermal gas pressure at the central plane ($z = 0$) and k is a damping parameter

| λ | Thickness (pc): k (m^{-1}) | | | Thickness without damping (pc) |
|-----------|---|------------|------------|--------------------------------|
| | 10^{-16} | 10^{-17} | 10^{-18} | |
| 0 | 0.20 | 0.20 | 0.20 | 0.20 |
| 10 | 1.32 | 1.97 | 1.87 | 1.84 |
| 20 | 1.74 | 3.70 | 3.56 | 3.49 |
| 30 | 1.99 | 5.19 | 5.29 | 5.13 |
| 40 | 2.17 | 6.47 | 7.04 | 6.77 |

$$\frac{d}{dz} \left(\tilde{\rho} + \lambda \sqrt{\tilde{\rho}} e^{-kz} \right) = -\sqrt{\frac{8\pi G \rho_0}{c^2}} \tilde{\rho} \sqrt{1 + \lambda - \tilde{\rho} - \lambda \sqrt{\tilde{\rho}} e^{-kz}}. \quad (66)$$

No analytical solution of this equation has been found but using the substitution $u = \sqrt{1 + \lambda - \tilde{\rho} - \lambda \sqrt{\tilde{\rho}} e^{-kz}}$, where $u = 0$ at $z = 0$, reduces it to

$$\frac{du}{dz} = \sqrt{\frac{2\pi G \rho_0}{c^2}} \left(\sqrt{\frac{\lambda^2}{4} e^{-2kz} + 1 + \lambda - u^2} - \frac{\lambda}{2} e^{-kz} \right), \quad (67)$$

which allows the problem to be solved numerically.

The mass and energy density ratio profiles given by an intermediate value of the damping parameter k (10^{-17}m^{-1}) are shown in Fig. 5, with the actual density profiles shown in Fig. 6. As in the case without damping, increasing the value of λ increases the thickness of the cloud but in addition it also accentuates the rise in density occurring either side of the central plane. The increase in density can be seen in the expression

$$\frac{d\tilde{\rho}}{dz} = \frac{kU - \rho_0 \tilde{\rho} g}{\rho_0 c^2 + U/2\tilde{\rho}}, \quad (68)$$

which is obtained from the equilibrium equation (Eq. 32) and the wave propagation equation (Eq. 31): a positive density gradient is given when $kU > \rho_0 \tilde{\rho} g$. This criterion is satisfied in a region near the central plane where the value of the wave energy density is at its maximum (Fig. 5(ii)). Clearly increasing the initial value of the wave energy density, i.e. increasing λ , will increase the extent of this region. Such a mass distribution is supported against gravity by an Alfvénic pressure which is essentially a zero-mass “material”. Rayleigh-Taylor instability may result and this is a point which will be discussed in future work where there is a more realistic distribution of Alfvén wave sources.

The actual thickness of the gas slabs represented by these profiles is shown in Table 2, the last column of which contains for comparison the results for a cloud supported by waves without any damping. The isothermal layers have column density $\mathcal{M} = 10^{-1} \text{kg m}^{-2}$ and temperature $T = 10\text{K}$, and thus from Eq. (63) the same central mass and energy densities as shown in Table

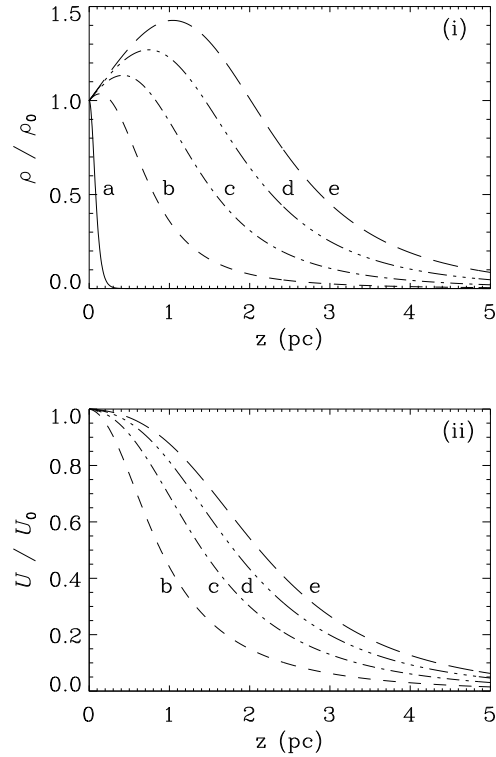


Fig. 5. The (i) mass density ratio and (ii) energy density ratio profiles in an isothermal gas slab supported by waves including damping, with column density $\mathcal{M} = 10^{-1} \text{kg m}^{-2}$, temperature $T = 10\text{K}$ and damping parameter $k = 10^{-17} \text{m}^{-1}$, for (a) $\lambda = 0$, (b) $\lambda = 10$, (c) $\lambda = 20$, (d) $\lambda = 30$ and (e) $\lambda = 40$; where $\lambda = U_0/\rho_0 c^2$ is the ratio between the wave pressure and the isothermal gas pressure at the central plane ($z = 0$)

1. Notice that increasing the value of the parameter k does not necessarily increase the size of the gas slab (see Fig. 7). If the damping is too strong then the wave is stopped well within the density distribution and the ability for these waves to provide any overall support for the gas is lost. And so for each value of k , increasing the value of the parameter λ will continue to increase the thickness of the layer but only up to a certain value at which the waves have been completely damped. Thus, introducing the damping has complicated the linear relationship between the thickness of the slab and λ (see Fig. 8) although the benefits of a low column density and high temperature are still prevalent.

4.3. Discussion

The values displayed in Table 2 show how the thickness of the slab varies with decreasing damping and then with no damping at all. A direct comparison between the support with damping and that without is illustrated in Fig. 9 for different values of the parameter k , from 10^{-16}m^{-1} for strong damping through to 10^{-18}m^{-1} for weak damping. It can be seen that when the waves are only weakly damped, the gradient in the wave energy density increases slightly, resulting in a small increase in cloud support and thus a marginally larger value for the thickness.

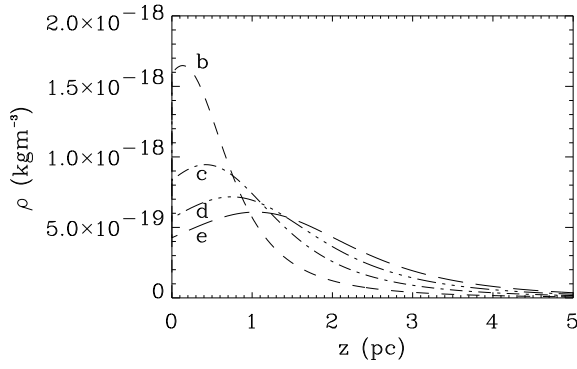


Fig. 6. The mass density profiles as for Fig. 5

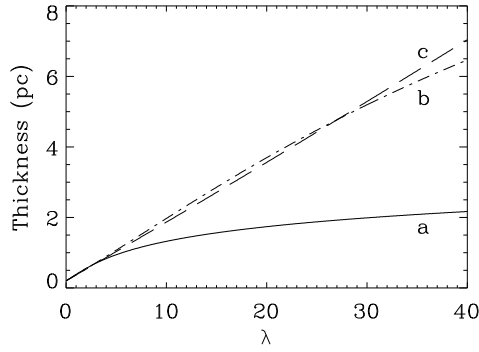


Fig. 7. The thickness of an isothermal gas slab supported by waves including damping, with column density $\mathcal{M} = 10^{-1} \text{ kg m}^{-2}$ and temperature $T = 10\text{K}$, plotted against the parameter λ for (a) $k = 10^{-16} \text{ m}^{-1}$, (b) $k = 10^{-17} \text{ m}^{-1}$ and (c) $k = 10^{-18} \text{ m}^{-1}$

However, if the damping is too strong then the thickness of the gas slab actually decreases relative to that without any damping. The upper limit of the parameter k ($\sim 10^{-16} \text{ m}^{-1}$), which gives the strongest damping, arises from considering the maximum wave frequency ω_{max} (see Sect. 3) as $k \propto \omega^2$. This is the limit at which there can be some coupling by friction between the ions and the neutrals. However, to achieve good coupling and hence support of the cloud as a whole the wave frequency $\omega \ll \omega_{\text{max}}$ and thus $k \ll k_{\text{max}}$, i.e. $k \ll 10^{-16} \text{ m}^{-1}$, which is advantageous for cloud support.

The second key parameter in determining the extent of the cloud support and hence the thickness of the layer is,

$$\lambda = U_0 / \rho_0 c^2 = b^2 / 2\beta B_0^2, \quad (69)$$

where the plasma beta $\beta = 2\mu P / B_0^2$ and $U_0 = b^2 / 4\mu$ (see Sect. 2.2.1). For a typical plasma beta of

$$\beta = 5.79 \times 10^{-3} \left(\frac{T}{10\text{K}} \right) \left(\frac{n_{\text{H}_2}}{10^9 \text{ m}^{-3}} \right) \left(\frac{B}{10^{-8} \text{ T}} \right)^{-2} \quad (70)$$

this parameter takes the value $\lambda \sim 85 (b^2 / B_0^2)$. However $b/B_0 \simeq v/v_A$, where v is the velocity associated with the magnetic perturbation b . Now the fluid velocity is supersonic

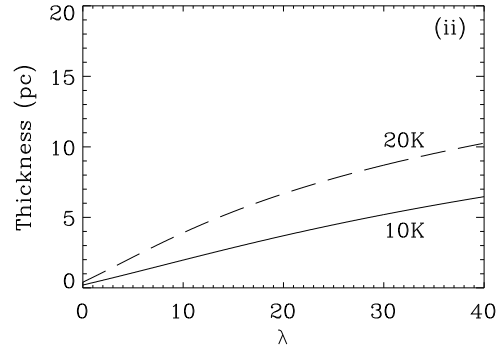
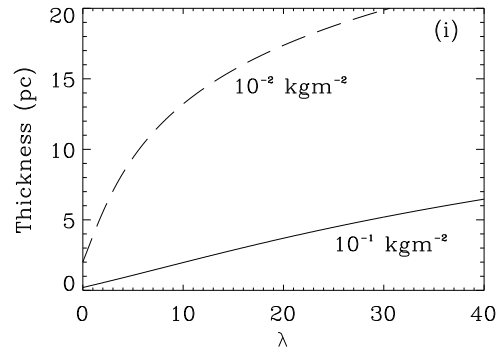


Fig. 8. The thickness of an isothermal gas slab supported by waves including damping, with $k = 10^{-17} \text{ m}^{-1}$, plotted against the parameter λ for (i) different values of the column density (\mathcal{M}) with temperature $T = 10\text{K}$ and (ii) different values of the temperature (T) with column density $\mathcal{M} = 10^{-1} \text{ kg m}^{-2}$

but subalfvénic ($v \leq v_A$) and typical values (see Sect. 1) of $v \sim 1 \text{ km s}^{-1}$ and $v_A \sim 4.5 \text{ km s}^{-1}$ give $\lambda \sim 20$, which corresponds to a cloud thickness of a few parsecs (see Table 2) akin to observations. For turbulent velocities approaching the Alfvén value (Myers & Goodman 1988; Goodman & Heiles 1994; Mouschovias & Psaltis 1995) the parameter $\lambda \sim 80$; in the case where there is no damping this would result in a continuous increase in the thickness as $z \propto \lambda$ (see Fig. 4). However, with damping included the resultant thickness of the layer would depend on the value chosen for the parameter k (see Fig. 7): the strongest value gives a thickness of only $\sim 2 \text{ pc}$, while an order of magnitude less gives $\sim 10 \text{ pc}$ (equivalent to a radius of $\sim 5 \text{ pc}$), which is in good agreement with observations of dwarf molecular clouds (e.g. see Shu et al. 1987).

In summary, it has been shown that Alfvén waves can provide the required support for a dwarf (or dark) molecular cloud along the magnetic field lines, while support perpendicular to the field lines is provided by the Lorentz force. The damping of these waves is not a necessary condition for this support, but weak damping is both likely and favourable.

5. Conclusion

This study has described a self-consistent model which successfully provides the necessary support for a molecular cloud

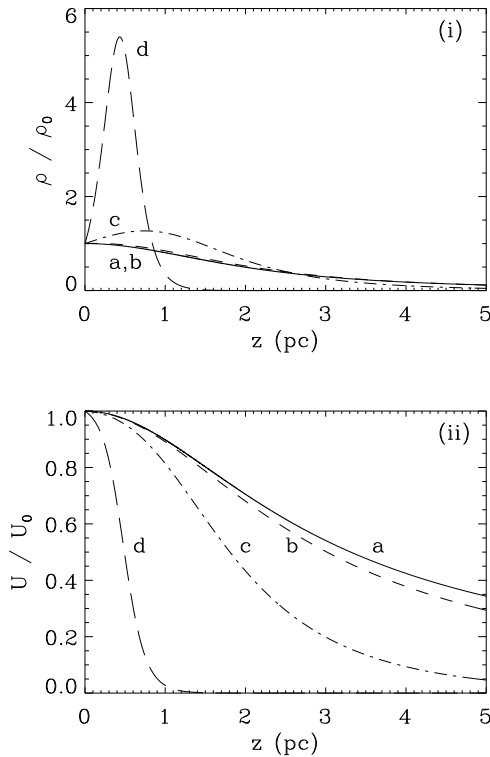


Fig. 9. The (i) mass density ratio and (ii) energy density ratio profiles in an isothermal gas slab, column density $\mathcal{M} = 10^{-1} \text{kg m}^{-2}$ and temperature $T = 10\text{K}$, with $\lambda = 30$ for (a) support by waves in the absence of damping, and support by waves including damping with (b) $k = 10^{-18} \text{m}^{-1}$, (c) $k = 10^{-17} \text{m}^{-1}$ and (d) $k = 10^{-16} \text{m}^{-1}$

parallel to the ordered magnetic field. The support is given by an Alfvén wave pressure force, the Alfvén waves being generated by the orbital motions of large condensations of gas within the cloud. In addition, utilising the magnetic field allows the observed linewidths and rotation within a dwarf molecular cloud to be understood (Arons & Max 1975; Shu et al. 1987; Mouschovias & Psaltis 1995). The assumptions made within this initial model are certainly simple when compared with the complexity of actual clouds, particularly on such aspects as the cloud’s thermodynamics, the distribution of wave sources and the one-dimensional geometry adopted for the model. Thus it would be premature to attempt a direct comparison between this model and observations. Nevertheless this work does provide a useful insight into the mechanical equilibrium found within dwarf (or dark) molecular clouds. It shows that realistic values of the magnetisation parameter (λ) result in significant mechanical support, even in the absence of damping; and that the idea of Alfvén wave support deserves further examination, which is presently being conducted on some aspects left aside in this paper.

Acknowledgements. C.E. Martin and E.R. Priest thank the United Kingdom Particle Physics and Astrophysics Research Council (PPARC) for financial support. The authors would also like to thank David Williams for useful discussions.

References

- Arons J., Max C.E., 1975, *ApJ* 196, L77
 Blitz L., Thaddeus P., 1990, *ApJ* 241, 676
 Bonazzola S., Falgarone E., Heyvaerts J., Péruault M., Puget J.L., 1987, *A&A* 172, 293
 Bonazzola S., Péruault M., Puget J.L., Heyvaerts J., Falgarone E., Panis J.F., 1992, *J. Fluid Mech.* 245, 1
 Crutcher R.M., Kazès I., 1983, *A&A* 125, L23
 Dewar R.L., 1970, *Phys. Fluids* 13, 2710
 Draine B.T., Roberge W.G., Dalgarno A., 1983, *ApJ* 264, 485
 Elmegreen B.G., 1979, *ApJ* 232, 729
 Falgarone E., Puget J.L., 1986, *A&A* 162, 235
 Farquhar P.R.A., Millar T.J., Herbst E., 1994, *MNRAS* 269, 641
 Fatuzzo M., Adams F.C., 1993, *ApJ* 412, 146
 Field G.B., 1978, *Conditions in Collapsing Clouds*. In: Gehrels T. (ed.) *Protostars and Planets*. University of Arizona Press, Tucson, p. 243
 Gammie C.F., Ostriker E.C., 1996, *ApJ* 466, 814
 Goodman A.A., Heiles C., 1994, *ApJ* 424, 208
 Gredel R., Lepp S., Dalgarno A., Herbst E., 1989, *ApJ* 347, 289
 Hartquist T.W., Rawlings J.M.C., Williams D.A., Dalgarno A., 1993, *QJRAS* 34, 213
 Hartquist T.W., Williams D.A., 1995, *The Chemically Controlled Cosmos*, Cambridge University Press, Cambridge
 Larson R.B., 1981, *MNRAS* 194, 809
 Le Bourlot J., Pineau des Forêts G., Roueff E., Flower D.R., 1993, *A&A* 267, 233
 McKee C.F., 1989, *ApJ* 345, 782
 McKee C.F., Zweibel E.G., 1995, *ApJ* 440, 686
 Moneti A., Pipher J.L., Helfer H.L., McMillan R.S., Perry M.L., 1984, *ApJ* 282, 508
 Mouschovias T.C., 1995, *Role of Magnetic Fields in the Early Stages of Star Formation*. In: Ferrara A., Heiles C., McKee C.F., Shapiro P. (eds.) *ASP Conf. Series, The Physics of the Interstellar Medium and the Intergalactic Medium*. San Francisco
 Mouschovias T.C., Psaltis D., 1995, *ApJ* 444, L105
 Mouschovias T.C., Spitzer L., 1976, *ApJ* 210, 326
 Myers P.C., Goodman A.A., 1988, *ApJ* 326, L27
 Norman C., Silk J., 1980, *ApJ* 238, 158
 Priest E.R., 1982, *Solar Magnetohydrodynamics*, D. Reidel Publishing Company, Dordrecht
 Scoville N.Z., 1992, *Interstellar Medium, Molecular Hydrogen*. In: Maran S.P. (ed.) *The Astronomy and Astrophysics Encyclopaedia*. Cambridge University Press, Cambridge, p. 373
 Shu F.H., 1983, *ApJ* 273, 202
 Shu F.H., Adams F.C., Lizano S., 1987, *ARA&A* 25, 23
 Spitzer L., 1968, *Diffuse Matter in Space*, Interscience Publishers, New York, 217
 Tiné S., Lepp S., Gredel R., Dalgarno A., 1997, *ApJ* (submitted)
 Yan M., Dalgarno A., 1997, *ApJ* (submitted)
 Young J.S., Scoville N.Z., 1991, *ARA&A* 29, 581
 Zuckerman B., Palmer P., 1974, *ARA&A* 12, 279
 Zweibel E.G., Josafatsson K., 1983, *ApJ* 270, 511